Sediment dynamic equilibrium, a key for assessing a coastal anthropogenic disturbance using geochemical tracers: Application to the eastern part of the Bay of Seine

Noémie Baux, Anne Murat, Quentin Faivre, Sandric Lesourd, Emmanuel Poizot, Yann Méar, Sébastien Brasselet, Jean-Claude Dauvin

Sediment dynamic equilibrium, a key for assessing a coastal anthropogenic disturbance using geochemical tracers: Application to the eastern part of the bay of Seine

Noémie Baux[a,*], Anne Murat[b,c], Quentin Faivre[b,c], Sandric Lesourd[a], Emmanuel Poizot[b,c], Yann Méar[b,c], Sébastien Brasselet [d] and Jean-Claude Dauvin[a]

[a] Normandie Univ, UNICAEN, UNIROUEN, CNRS, Morphodynamique Continentale et Côtière (M2C), UMR CNRS 6143, 14000 Caen, France

[b] Normandie univ., UNICAEN, Laboratoire des Sciences Appliquées de Cherbourg, EA 4253, 50100 Cherbourg, France

[c] Conservatoire National des Arts et Métiers, INTECHMER, 50100 Cherbourg, France

[d] Grand Port Maritime du Havre (GPMH), 76067 Le Havre, France

*Corresponding author: Email address: noemie.baux@unicaen.fr (Noémie Baux)

Abstract

Geochemical studies are becoming more and more frequent in the context of the increasing pressure of human activities on marine coastal ecosystems and represent an appropriate tool to assess anthropogenic disturbances. Moreover, it is difficult to find discriminant markers. The eastern part of the Bay of Seine (English Channel) is highly impacted by the presence of harbour activities, fishing and sediment extraction. Dredged sediment from the Grand Port Maritime du Havre (GPMH) are deposited at the subtidal Octeville site, in the north-eastern part of the mouth of the Seine estuary (mixed sediment area). To understand natural and anthropogenic sedimentary mechanisms in this area, a geochemical and sedimentological study was conducted at the beginning of 2016. A dense sampling campaign including 179 stations was carried out between Cap de La Hève and Cap d'Antifer. For comparison, sampling was carried out in the harbour (13 samples in basins strongly or very weakly dredged), in the dredged grab itself and in the Seine estuary sediment (one station in the brackish zone and two stations in the river freshwater zone). Elemental compositions were determined by X-Ray Fluorescence spectrometry and infrared spectrometry. Using PCA (Principal Component Analysis), seven constituents were selected (Si, As, S, Pb, Rb, organic Br and TOC) to determine the area influenced by dumped spoil and the sediment transport directions. Sediment areas in dynamic

equilibrium display a TOC gradient perpendicular to the coastline, linked to granulometric variations due to a combination of the swell and tidal currents. In the study area, dredged sediment are finer grained and have undergone changes due to the influence of diagenetic processes characteristic of the harbour environment. As a result, these sediment are enriched in sulphides, Pb, TOC and Rb, which allows us to highlight the in-situ deposited sediment spoil. Dumped sediment and the area subject to their influence are clearly identified since they locally disrupt the natural dynamic equilibrium state.

Keywords: Sedimentary dynamic equilibrium, geochemical tracers, X-Ray Fluorescence spectrometry, dredged sediment spoil, Bay of Seine.

1. Introduction

The concept of dynamic equilibrium was introduced for the first time by Gilbert (1877), in the context of a geological survey in the United States (Henry Mountains, Utah, USA), to refer to any change in a system which adjusts over time in order to minimize the effect of the changes (Bracken and Wainwright, 2006). Dynamic equilibrium in coastal marine sedimentary studies is also defined as an equilibrium between particle transport, erosion and deposition as a function of physico-chemical-biological and hydrodynamic parameters (Perillo, 1995). The transport and deposition of fine particles are controlled by two marine forcing parameters: tidal currents and swell. In the case of a macrotidal regime, these forcings create an area where the marine and fluvial particles are strongly mixed under the effect of strong tidal currents and swells. In coastal areas, fine particle deposition and erosion processes are mainly based on studies of sedimentological features, the calculation of sedimentation rates and their association with benthic macrofauna (Christie et al., 1999; Dyer et al., 2000; Méar et al., 2006; Lesourd et al., 2016; Murat et al., 2016).

However, identifying the provenance of fine sedimentary material is a difficult task (Dubrulle-Brunaud, 2007). Sediment source-areas and the description of markers are also represent challenging topics commonly addressed in studies on the origin and transit (deposition and suspension) of particles. Some authors focus exclusively on clay minerals to highlight sedimentary dynamics in coastal areas (Oliveira et al., 2002), while other studies make use geochemical tracers as markers of sedimentary material, mainly with the aim of assessing contamination/pollution (Goldberg et al., 1979; Macdonald et al., 1991; Lee and Cundy, 2001; Santschi et al., 2001). In the Bay of Seine and Seine estuary, several studies have used

geochemical or biomarkers to elucidate the origin of fine material (Dupont et al., 1994; Dubrulle-Brunaud, 2007; Dubrulle et al., 2007; Vrel, 2012). These studies in the Seine estuary highlight the existence of four sources (marine, fluvial, inherited sediment and estuarine) which contribute to particulate mixing and point out the difficulty of differentiating these sources with geochemical markers (Dubrulle-Brunaud, 2007). The present study focuses on the eastern part of the Bay of Seine, between the Cap de La Hève and Cap d'Antifer, including the dumping site used by the Grand Port Maritime du Havre (GPMH). The area studied here includes a fifth potential source, corresponding to fine sediment dredged from harbour basins which is then dumped offshore.

Harbours need carry out periodically dredging to maintain sufficient water depth in the basins and access channels for the purpose of navigation and port activities. The dredged sediment can be deposited onshore or, in cases where they do not contain hazardous products, can be dumped at sea (Marmin et al., 2014, 2016). Nevertheless, marine dumped sediment may have different physical and chemical characteristics, which then generate multiple effects on the physical environment: input of fine particles, decreasing water depth and modification of bottom sediment (Chauvin et al., 1986; Boutin, 2000; Smith and Rule, 2001; Marmin et al., 2016).

The objective of this study is to understand the functioning of natural sedimentary processes in the study area and determine the impact of dumping as well as the consequences of harbour sediment inputs in this coastal area, while developing a new approach associated with the use of geochemical tracers.

2. Study area

2.1. General context

The study area is located in the eastern part of the Bay of Seine in north western France (English Channel), between Le Havre harbour and Antifer harbour (Fig. 1).

The study area has a maximum water depth of 30 m and a mean depth of 15 m. The site is characterized by a macrotidal regime, with a tidal range of 7.5 m during spring tide, showing a strong maximum turbidity zone compared to other macrotidal estuaries (Le Hir *et al.*, 2001a). Tidal currents trend mainly to the northeast (NE) during flood tide and to the southwest (SW) during ebb tide. The residual current flows towards the NE. Northwesterly winds are generally present throughout the year (mean speed of about 7 m s^{-1}, with maximum speed >15 m s^{-1}), but show maximum force between November and March.

Water circulation in the eastern Bay of Seine is determined by the general trend of tidal currents. Nevertheless, the shoreline greatly disrupts this general pattern. At the beginning of flood tide, the Antifer current runs along the coastline and turns towards the Seine Estuary. At the end of the flood tide, the current is reversed (Verhaule current) and flows towards the NE, but still follows the coastline. At the ebb, a new reversal of the water flow occurs, with the current directed towards the SW (Larsonneur, 1971; Le Hir et al., 2001a; Méar et al., 2006).

The Seine estuary is a major source of fine particles in the eastern part of the Bay of Seine and in the harbour basins of Le Havre. The average annual discharge of the Seine is estimated at 435 m^3 s^{-1}, rising to 534 m^3 s^{-1} over the last decade. The minimum discharge is generally observed between August and October and the maximum discharge between November and April. Since 1941 (first measurements), with 2001 showing the highest average annual discharge (903 m^3 s^{-1}). Average weight concentrations of suspended particulate matter (<100 µm) in the estuary of the Seine (measurements carried out at Poses) are close to 30 mg l^{-1}(Le Hir et al., 2001b). The average input of fine particles supplied by the Seine is 6 10^5 t y^{-1} (ranging between 1.3 10^5 t y^{-1} and 1.7 10^6 t y^{-1}; Lesourd et al., 2016). Along the coast, the turbidity plume from the Seine estuary develops over a width of one kilometre, even in the absence of waves (Brylinski et al., 1991). The deposited mud is unconsolidated and thus easily resuspended by tidal currents (Avoine and Larsonneur, 1987; Lesourd et al., 2003; Ubertini et al., 2012). In terms of clay minerals, the Seine estuary corresponds to a mixing zone between continental clays composed mainly of smectites and kaolinites and marine clays composed mainly of illites and chlorites. (Lesourd, 2000). This assemblage of clay minerals is stable in the estuary, both upstream and downstream (Dubrulle et al., 2007).

The seafloor of the study area is mainly covered by muddy sands, with sandy muds, sands and pebbles along the coast (Lesourd et al., 2016). Previous studies have highlighted, between Cap de La Hève and the Cap d'Antifer, a coastal fringe with the fine fraction (<63 µm) making up 10 % to 25 % of the sediment, but with spatial and temporal fluctuations in the mud content (Avoine et al., 1981; Crevel, 1985; Larsonneur et al., 1985; Méar et al., 2018). In 2014, studies conducted by the Havre harbour authorities in an offshore area near the Octeville dumping site showed silt and clay contents (<63 µm) varying from 4.9 % to 48.8 % in the northern zone between the dumping site and Antifer (mean value 29.5 %) and 14.9 % to 37.7 % (mean value 27.4 %) in the southern zone between the dumping site and Le Havre (Brasselet, 2014).

2.2. Le Havre harbour

Le Havre harbour was built in 1517 as a military and commercial port. It was the 58th largest world port in 2013 and the second French port in 2014, with a traffic of 67,574,000 tons.

In this study, the harbour is divided into three large distinct zones (Basselet, 2014; Fig. 1):
- Slightly dredged basin and canal located on either side of a lock with little harbour activity. The basins are dredged only every 2 to 3 years (<15 000 m^3). The basins on the other side of the lock are not subject to the tide (1 m maximum tidal range). There is not direct communication with the Seine estuary and little water renewal. Sediment are mainly composed of sandy mud and muddy sand (53.4 % <63 µm on average for 2009 to 2014 period).
- The historical harbour (Port Ancien), which was the main harbour before the Port 2000 development in 2002-2005, is still used today but with a reduced level of maritime activities. In 2014, the dredged volume was 584 763 m^3. Sediment are mainly composed of fines (on average, 82 % <63 µm fraction for 2009-2014).
- The new harbour (Port 2000), which represents an expansion of the historical harbour, was built from 2002 to 2005 (with latest construction of dykes in 2009) and has been in use since 2006. This new part of the harbour handles a great amount of maritime traffic, with large container ships (capacity of up to 20 000 containers).

The average volume dredged is 2 10^6 m^3 y^{-1}. Sediment are mainly composed of mud (on average, 79.9 % <63 µm fraction for 2009-2014).

In this study, samples were collected from these three different zones to represent the "source sediment", to determine the sediment composition and compare the dredged material with dumped sediment.

2.3. Octeville dumping site

Since 1947, the Octeville dumping site has been used by the GPMH (Grand Port Maritime du Havre). Located 8 km from Le Havre, the site was chosen for its proximity to the harbour and the strong hydrodynamics in this zone, which leads to the natural dispersal of fine particles. The dredged sediment results from daily harbour maintenance and represents approximately 2.5 to 3 10^6 m^3 y^{-1} since 2006, following the harbour extension works (Port 2000). Before this extension, dredged volumes represented 1.3 10^6 m^3 y^{-1}. The dumped sediment are strongly heterometric. Mud accounts for 70 % of the sediment at the dumping site (average of fine fraction (<63 µm): 77.5 %, in 2014, Brasselet, 2014). But the strong hydrodynamic regime causes resuspension of finer sediment which are dispersed outside the dumping area over large distances, mainly towards the NE (Auffret and d'Ozouville, 1985a,b; Crevel, 1985; Chauvin et al., 1986).

The seafloor of the dumping site is covered with muddy sand and sandy mud in the northern and western part of the site and with gravel and pebble in the southeast (SE). The SE sector of the site corresponds to a historical deposition area associated with a shoal (-5 m with respect to minimum sea level in Le Havre harbour = Cote Marine du Havre, CMH). The dumping strategy of GPMH has evolved over time to minimize impact. Currently, sediment are deposited to the N, NW, and SW of the dumping site, according to a system of "boxes", in which the sediment is distributed in a thin layer (elevation of between 0.1 to 0.6 m per box per year).

3. Methodology

3.1. Sampling strategy

A sampling of 179 stations (regular grid, distance of 500 m between stations) was conducted in January and February 2016 (on 19, 20, 21 January 2016, with tidal coefficients of 56 to 72; and on 13 February 2016, with a tidal coefficient of 94) using a 0.04 m^2 Shipeck grab aboard the GPMH vessel “Le Marais”, between the Cap de la Hève and the Cap d’Antifer (Fig. 2, zoom 3). A visual examination of sediment composition and granulometry was carried out for each grab (notations and photos), then a sample of the surface sediment and, finally, a sample of the whole grab was collected and stored in plastic bags.

In addition, samples from the harbour basins (same sampling method as described above) were also studied. To obtain a good knowledge of the geochemical and sedimentary parameters of the superficial sediment in harbour basins (dumped sediment), samples were collected from strongly dredged and slightly dredged basins: four samples from strongly dredged basins in the historical harbour and Port 2000 (H5, H8, H21 and H2000; 24 March 2016; Fig. 2, zoom 2), four samples from very slightly dredged basins in the historical harbour (tidal influence) and the canal on the other side of a lock (H22, H11, HG1 and HDO; 10 May 2017; Fig. 2, zoom 2).

Moreover, sampling was carried out on the dredge grab itself, to obtain information on deeper dredged sediment (reduced sediment): one sample with three replicates from the historical harbour: HD1, HD2 and HD3 (6 October 2017) and one sample with two replicates from Port 2000: HD4 and HD5 (26 October 2017; Fig. 2, zoom 2).

To determine the composition of sediment in the Seine estuary, three samples were also collected (Fig. 2, zoom 1): one station in the brackish zone (T1; 24 March 2016) and two nearby stations in the freshwater section of the river (B1 and B2; 6 March 2017).

Bottom currents measurements were conducted by the GPMH from June to November 2012 (localisation of points on Fig. 1). The current velocities and directions were measured at six

stations with an ADCP instrument (Current Profiler with Doppler Effect 600 kHz). The duration of data acquisition was fixed at one tidal cycle (12 hours) and two measurements were performed per station (at spring and neap tide). The ADCP was placed 2 m above the seabed.

3.2. Laboratory analyses

After collection, all samples were frozen in the laboratory before sedimentary and geochemical analyses. The sedimentary data obtained are used to check and support the interpretations based on geochemical data.

To assess sediment granulometry, laser diffraction particle-size analysis was carried out on fine superficial sediment collected by Shipeck grab (parameters used: measured interval: 0.02 µm to 2 mm. Real part: 1.54 and imaginary part: 0.1. Mie diffraction method).

Elemental contents were determined by X-ray fluorescence and Total Organic Carbon (TOC) was analysed on superficial sediment collected by the Shipeck grab. Frozen samples were freeze-dried. The coarse fraction was removed with a 2-mm sieve. The weight of the sample was reduced to obtain 10 g aliquots using a manual quartering method (random separation of sample aliquots). Tests were performed beforehand to select the best method to conserve as much material as possible for the elemental analyses (either crush then rinse or rinse then crush, with varying intensity and duration). The results reveal the loss of a certainamount of potassium and rubidium when samples are rinsed before crushing. Also, samples were crushed then rinsed to avoid rubidium and potassium loss.

Sediment samples were acidified by H3PO4 (1 M), to remove carbonates, dried on a hot plate at 40° C and measured for TOC content by combustion in a LECO CS 744 carbon sulphur analyzer. Two or three replicates of dried and homogenized sediment (50 mg) were analysed per sample. The results of organic carbon measurements are expressed in percent of dry sediment. The precision determined from replicate subsampling was ±0.05% organic carbon.

The methodology chosen for sample preparation consisted of grinding freeze-dried samples (10 g) for 3 min at 600 rpm (revolutions per minute) with an automatic grinder, then sub-sample were rinsed with ultra-pure water in a centrifuge (3x15 min at 300 rpm), to remove residual salt due to the evaporation of marine pore-water. This rinsing was carried out to obtain sulphide without sulphate, as well as bromine bound to organic matter without contamination from the bromide (Br) contained in seawater. Previous studies have shown that pure water only removes Br to the extent expected for evaporated pore waters (Mayer et al., 1981, 2007) and that insignificant organic bromine is washed away (Mayer et al., 2007). The samples crushed and

rinsed in this way were freeze-dried again and analysed by X-Ray Fluorescence using an xSORT instrument (elements from Si to U). The instrument was set up on a stand and analyses were performed with the manufacturer's Environ-H program. Ground sediment were manually compacted and placed in a 15-mm-diameter plastic cup with a 4-µm-thick polypropylene window. For each sample, four replicates were analysed with a counting time of 300 s The detection limits of each elements are vary according to the atomic mass.adjusted according to the calibration line. For the lightest element, Si the detection limit is 5000ppm. For the As and the elements heavier the detection limit is 5ppm. Accuracy of measurements is poor at the detection limit and increases with the concentration. The replicates values generally agree within 5 %. But for Si, the lighest element, they can sometimes agree only within 10%. To calibrate the results, 25 marine sediment samples were used. These samples were analysed by ICP-AES ("Service d'analyses des roches et minéraux", SARM-Nancy, France). For Br calibration, we used standards prepared from Mediterranean sediment. The sediment was sieved with mesh width of 40 µm and high purity water, freeze-dried, crushed and homogenized. Known quantities of KBr solution were added to the sediment sub-samples, and the sub-samples were freeze-dried, crushed and homogenized.

Following the analyses, a database was created for each station, with contents of elements (from Si to U), TOC and particle-size data. 163 samples were analysed from the study area, as some stations are composed of coarse sand and pebbles (especially the coastal stations). All the harbour and estuary stations (16 stations) were analysed. A total of 1074 analyses [716 XRF analyses (four replicates) and 358 TOC analyses (two replicates)] were performed on samples from 179 stations.

3.3. Data treatment

To describe the sedimentary functioning of the study area and highlight the possible impact of the dumping site, PCA (Principal Components Analysis) was conducted with R.3.4.1 software, as well as the FactoMiner and PerformanceAnalytics packages. PCA is one of the most commonly used multivariate ordination methods for establishing correlations between variables and samples. It is also used for performing data reduction of vibrational spectra and visualization of potential groupings between samples (Pearson, 1901; Hotelling, 1933; Syms, 2008; Lewis and Menzies, 2015). For each PCA, two graphical representations are obtained (one for variables, the other for samples). Also, several consecutive PCAs (7 in number) are conducted to eliminate non-informative or redundant items, according to the contents of each element in each sample,

correlations, interaction and distribution between variables/elements, as well as spatial representation of variables/elements and individuals/samples. The data are not standardized to study the impact of particle size and sedimentary dynamics.

Cartographic analyses were carried out with ArcGis 10.2.2 software to facilitate geographical visualization of the results and support the interpretations

4. Results

4.1. Selected geochemical parameters

In this study, it is necessary to simplify the data to obtain parameters which express the variability of the sample pool and account for the functioning of the study area. With xSORT, 18 calibrated chemical elements are measured for each station (Si, S, K, Ca, Ti, V, Mn, Fe, Ni, Ga, As, Organic Br (denoted BrOrg), Rb, Sr, Y, Pb, Th and U). Analyses were performed step by step to gradually reduce the number of geochemical parameters, to select the best markers for discriminating samples from each other. In fact, it is difficult to discriminate between samples from the Bay of Seine, harbour basins and Seine estuary (brackish water) because they are very similar due to a mixing of particles. Since Le Havre harbour is located in the northern part of the Seine estuary, its basins are filled with sediment very similar to those naturally present in the Bay of Seine. Finally, only seven discriminant constituents are retained in the last PCA: Si (silicon), S (sulphide), As (arsenic), BrOrg (organic bromine), Rb (rubidium), Pb (lead) and TOC (total organic carbon).

Rb is a marker of clay minerals, especially illites (Reynolds, 1963), which are naturally present in the Seine estuary at abundances of 15-20% (Lesourd, 2000; Dubrulle et al., 2007; Vrel, 2012). Rb shows a constant level in the estuary, with Enrichment Factor = 1 (Dubrulle et al. 2007). This element is preferentially retained in weathered illites in comparison to K (Garrels and Christ, 1965; Mahjoor et al., 2009).

BrOrg and TOC are quantitative markers of organic matter content. They are correlated which each other and their ratio is an indicator of terrigenous versus marine organic matter (Price and Calvert, 1977; Mayer et al., 1981, 2007; Leri et al., 2010, 2014).

Si marks the coarse detrital fraction, especially quartz and flint in the Bay of Seine (Dubrulle-Brunaud, 2007).

Arsenic (As) appears to be a marker of coastal glauconite-rich sediment (greenish sand). Arsenic is naturally present in geological materials and, even though it is not described as a major component of glauconite [Fe-rich alumino silicate; McRae (1972) and Banerjee et al. (2016)], it

can be taken up during "glauconization" and can be found in illite-rich glauconite (Mumford et al., 2012). Moreover, the presence of As in glauconite is well demonstrated because this element can be assimilated by microbial activities and released into the water from geological materials (Barringer et al., 2001, 2010). In the Bay of Seine, glauconites formed during the Aptian-Albian have been described offshore and to the west of Cap d'Antifer (Larsonneur et al., 1975). However, only few studies report the presence of arsenic in glauconite from the Bay of Seine.

Sulphide (S) is characteristic of sulphide-rich harbour sediment. Harbour basins contain sediment with high levels of organic matter, the driving force for most primary diagenetic redox reactions (Kasten and Jørgensen, 2000). Mineralization of organic matter is carried out by microorganisms which preferentially consume oxygen. However, the supply of oxygen from sea water to harbour sediment is limited, and the low oxygen concentration in bottom waters combined with high organic matter flux creates anoxic conditions (oxygen consumption by aerobic respiration). The sulphate reduction process becomes predominant because of the availability of high concentrations of sulphate in seawater, which leads to the production of sulphides in sediment (Jørgensen, 1977; Bo Barker, 1977).

Pb is present in large quantities in the Seine estuary (>100 ng l^{1}) and has the ability to be easily and rapidly fixed to sulphides (Cossa et al., 1993). Pb is precipitated in the sulphate reduction zone as sulphide minerals below the redox-cline, and may show enrichment at depth (Shaw et al., 1990; Spencer et al., 2003).

4.2. PCAs results

The results reported here concern the final PCAs performed with the seven selected geochemical parameters (Si, S, As, BrOrg, Rb, Pb and TOC). For the general PCA that includes all the samples, plane 1-2 accounts for 87.67 % of the total variance of the data scatter plot (Fig. 3). The similarity between the scatter plot of the first and this last PCA reflects a simplification of the data pool without loss of information. Interpretation of this result is described step by step in the following.

4.2.1. Relationships between elements

The correlations between the seven elements are illustrated spatially in Fig. 3A and numerically in Fig. 4. Four groups of variables can be identified. (1) The first group comprises Rb, TOC and BrOrg, which are strongly and significantly correlated with each other (r = 0.84-0.90).

(2) The second group includes S and Pb, two elements associated in the harbour sediment matrix and which also show a strong and highly significant correlation (r = 0.96). (3) The third group is represented by a single element, arsenic, which exhibits moderate positive but significant correlations with all other elements (r = 0.31-0.66). (4) The last group corresponds to Si, negatively correlated with markers of clays and organic matter (TOC, Rb and BrOrg) and positively correlated with As.

The anticorrelations between Si and Rb, TOC and BrOrg in the first group, reflects grain-size effects: sands are Si-rich and fine sediment have high clay and organic matter contents.

4.2.2. Relationships between samples

Fig. 3B illustrates the sample relationships. The scatter plot is J-shaped, with three elongate fields of data points, identified by a colour name.

(1) The "Red group" extends over the largest range (coordinates: 0 to 9 on axis 1 and -2 to 2 on axis 2), although it does not contain the largest number of samples (N = 26). The scatter plot shows a larger range on axis 1 than axis 2. This elongation trend occurs towards S and Pb. Samples of this group correspond to the finest sediment (rich in Rb, TOC and BrOrg), with a great variability of sulphide and lead contents.

(2) The "Blue group" includes most of the samples (N = 120), although the field of data points is the less extensive (coordinates: -2 to 0.5 on axis 1 and -2 to 1 on axis 2). Unlike the Red group, the range of data points is the same on axis 1 and axis 2 , with the scatter plot oriented according to variations in BrOrg and TOC.

(3) The "Green group" is the smallest (N = 23) and the elongation is less pronounced (coordinates: -2 to 1 on axis 1 and -1 to 5 on axis 2). The scatter plot is essentially oriented according to axis 2, being controlled by the Si and As variables. Samples of the Green group correspond to Si-rich coarse sediment, with glauconite enrichment in some samples.

4.2.3. Gradients and dynamic tracers

As previously described, Rb, TOC and BrOrg are quantitative markers of clays minerals and organic matter. These three correlated elements (Fig. 4 and 5B) show high concentrations in the finest sediment (Fig. 5A and Table 1). This clearly reflects sorting by particle size, which is supported by the scatter of data points along axis 1, with organic-poor sands to the left of the

graph and organic-rich clays to the right (Fig. 3). To interpret the patterns of the three data point clouds, we need to consider the raw dataset and the geographical origin of the samples.

- **Red group**

The Red group includes the finest samples (mean grain size of 62 µm) with the highest organic matter and clay contents (mean TOC of 1.80 %, mean BrOrg of 95 ppm and mean Rb of 75 ppm; Table 1). Samples included in this group correspond mainly to sediment collected in the harbour (surface and deeper sediment), the estuary and within or near the dumping site (dumped sediment). The gradient observed in this group is highlighted by the presence of six discrete sub-groups named "Red 1" to "Red 6" (Fig. 3B and Table 1). We observe a gradual decrease in contents of Pb, S, Rb, BrOrg and TOC from Red 1 to Red 6 (Table 1).

Red 1 is composed of seven samples (HD1, HD2, HD3, HD4 and HD5) collected by dredge grab in the historical harbour and Port 2000; HDO and H22 were sampled in slightly dredged basins on both sides of the lock (Fig. 1 and 2).

Red 2 consists of three stations (H11 and H8 sampled in the historical harbour, and 63 which is a station sampled in the southern dumping site). Red 3 corresponds to H21 (sampled in the historical harbour, close to outlet of a waste-water treatment plant). Red 4 corresponds to a mixing of harbour samples (HG1, H5 and H2000), samples within or near the dumping site (samples 119, 33 and 164) and one station sampled in the fresh-water section of the Seine estuary (B1). Red 5 is composed of stations in or near the dumping site (samples 50, 86 and 139) and one station in the brackish part of the Seine estuary (T1). Finally, Red 6 is made up solely of stations sampled within the study area (samples 22, 32, 35 and 137).

Harbour basins are calm hydrodynamic areas favourable for the accumulation of organic-rich fine sediment. Sulphate reduction occurs following burial and through the course of time, and the sediment becomes enriched with sulphide and lead. Thus, all the dredged samples belong to the Red 1 sub-group. Harbour superficial sediment are deposited in less anoxic conditions, so samples from that source plot within sub-groups Red 1 to 5. The dumping site receives harbour sediment of various origins. Furthermore, there are high-energy hydrodynamic conditions and oxygen-rich environments in the dumping area.

Anoxic dumped sediment are quickly reoxygenated and lose part of their fine fraction content. Samples collected in the dumping area belong to Red 4 to 5. Particles transported away from dumping site are exposed much longer to the high-energy environment. Samples taken outside the dumping area are in sub-groups Red 4 to 6.

The gradient from Red 1 to Red 6 reflects both changes in the energy level of the environment and the oxidation state of sedimentary particles. Harbour sediment that were initially buried progressively lose their geochemical specificity when introduced into the open marine environment.

- **Blue group**

The Blue group includes most of the samples, although its surface is the less expanded. The scatter plot is very compact (Fig. 3B). To improve our understanding of the origin of the elongated distribution of points on the scatter plot, we carried out a further PCA, referred to here as blue PCA, on the 120 individual samples falling in the Blue group, applying the same seven variables (Fig. 6).

In this “blue PCA”, plane 1-2 accounts for 74.09 % of the total variance of the data. Correlations are similar to those obtained from previous PCAs. BrOrg, TOC and Rb are again strongly correlated (BrOrg-TOC r = 0.74; BrOrg-Rb r = 0.87 and TOC-Rb r = 0.86) and Si is anticorrelated with Rb, BrOrg and TOC (r = -0.54 to -0.65). Pb, S and As have a very limited influence on the distribution of points. The blue PCA yields an impressive linear scatter plot, revealing an indisputable gradient of organic matter and clay mineral contents for the majority of samples. This gradient is characteristic of the Blue group, resulting from the adaptation of sedimentary deposits to the environmental energy level. Some constituents such as clays and organic matter are sorted according to their granulometric characteristics (in the present case, the fine grain-size class). The geochemical markers of these constituents can be regarded as dynamic tracers.

The other samples, plotting off the gradient line, are enriched in Pb and S or As. Granulometric sorting is again supported by the distribution of data points along axis 1, with sandy samples enriched in Si plotting to the left and more muddy samples enriched in Rb, TOC and BrOrg to the right (Fig. 6). It is noteworthy that all samples falling on this gradient are located outside the dumping site. To illustrate the variability of the Blue group on the cartographic application and better understand the mechanisms controlling the behaviour of these samples, we applied an artificial subdivision of the scatter plot. Four sub-groups were separated and named "Blue 1" to "Blue 4", (Fig. 3B, for graphical description and Table 1 for mean contents of the geochemical parameters). The gradients of TOC, BrOrg and Rb are again highlighted by the variation of numerical values (Table 1).

- **Green group**

The Green group is composed of coarse sandy sediment (mean grain size of 257 µm; Table 1). Samples of this group are enriched in Si. Two sub-groups are distinguished (Green 1 and Green 2). Green 1 is enriched in Si (mean abundance of 33.93 %), reflecting the increase of quartz and flint in these samples. Green 2 is enriched in Si, As and Rb (mean contents of 35.53 %, 10 ppm and 47 ppm, respectively; Table 1). Samples of this sub-group are located in the coastal area and contain glauconite (marked by an increase in As and Rb). The sediment are probably derived mainly from continental inputs due to cliff erosion. From 1985 to 2008, erosion from the top of the cliffs is estimated at 0.18 m y^{-1}, while erosion at the top of the footslope is estimated at 0.10 m y^{-1}. The intense erosion and accretion dynamics of the base of the cliffs removes large amounts of chalk and flinty clays and transports them out to sea (Elineau, 2013). Glauconite also comes from outcrops of Alptian-Albian sediment that were excavated to create the harbour navigation channel.

4.2.4. Cartographic representation of results

Fig. 7 shows a cartographic representation of the main geochemical PCA. Samples are represented by colours according to their group or sub-group shown on Fig. 3B. It is possible to delimit several sandy areas. (1) The first area is located in the sub-littoral zone (essentially Green 2 sub-group), with sediment being mainly enriched in Si, As and Rb (Table 1). This area is controlled by swell action, with coarse sediment devoid of fine fraction and containing glauconite. (2) The second area is located offshore in both the NW and SW parts of the study area (Green 1 and Blue 4 sub-groups). This area is mainly influenced by tidal currents. Samples are Si-rich (Table 1) and correspond to clean sands. (3) Other sandy areas located between the historical spoil dome and the coast (between the Cap de la Hève and the dumping site), where the energy is higher (current measurements at points 2, Fig. 1 and Table 2). The shallowing of the seabed at the historical dumping site (up to 5 m CMH) and its proximity to the coast creates a narrowing zone where the currents are accelerated (channelling of tidal currents) and erosion of the substratum is substantial.

On the other hand, we can also distinguish two muddy areas (Blue 1 sub-group and Red group). (1) The first muddy area is located within and around the dumping site. The dumping area is characterized by the presence of fine sediment enriched in BrOrg, TOC, Rb, S and Pb (Table 1). Due to the action of currents, fine sedimentary particles in the dumped spoil are progressively reworked, reoxidized, spatially redistributed and mixed with naturally introduced particles. An enrichment in fine sediment is noted towards the SE, but its origin is undetermined. It could

correspond to the transport of the dumped sediment back towards the harbour or the driving of estuary or dredged navigation channel sediment in the direction of the dumping site. Since the geochemical markers of these two sources are similar, it is not possible to differentiate between them. (2) The second muddy area is identified in the N-NE (only Blue 1 sub-group). Sediment are composed of a sandy mud mixture and exhibit a moderate TOC enrichment compared to the surrounding deposits (Table 1).

We note the occurrence of two particular points rich in TOC and BrOrg, corresponding to sample 137 in the Antifer basin and sample 164 along the coast close to the Cap de la Hève, which plot in the Red group (sample 137: 1.05 % TOC and 65 ppm BrOrg; sample 164: 1.87 % TOC and 97 ppm BrOrg). The enrichment in organic matter in sample 137 is easily explained because of its geographical position, Antifer harbour is a quiet hydrodynamic area favourable for the deposition of organic-rich fine sediment. Sample 164 is rich in organic matter (higher content than the mean of the Red group; Table 1), but is also As-rich (10 ppm, value close to the Green group mean), Pb (20 ppm) and Rb (75 ppm). Such a composition is unexpected in this area and, in addition, temporal monitoring in the study area (results not presented here) shows that the group attribution of this location changes according to the sampling period (Green group in August and Blue 4 sub-group in October). It is likely that this location corresponds to an old compacted mud area occasionally exposed due to strong erosional currents and sometimes covered by sands undergoing transit.

Finally, some samples show outlier values (Fig. 3 and 7, white hatched), that are confirmed by additional replicate analyses. These samples yield particular values in Si, As or BrOrg or show particular sedimentary facies.

5. Discussion

Three dynamic tracers (Rb, BrOrg and TOC) are potentially available. Rb marks clay minerals but is also enhanced in the coastal glauconite-rich sands. Consequently, it is not possible to use Rb as a dynamic tracer over the entire area. TOC and BrOrg both quantify organic matter, but TOC is the most widely accepted parameter, and it is chosen preferentially. The cartographic representation showing the increasing gradients in TOC (Fig. 8) reveals two different patterns: (1) areas with a structured gradient pattern linked to the bathymetry and (2) areas with gradients unrelated to bathymetry. The first pattern can be regarded as indicating that an area has reached dynamic equilibrium, with a sedimentary state in accordance with the hydrodynamic energy field. The second pattern reflects a disordered gradient distribution that indicates a disturbance.

5.1. Dynamic equilibrium

In the NE sector, two increasing TOC gradients can be identified which run perpendicular to the isobaths. The TOC values increase from offshore (25 m) to the 15 m isobath (Table 1) and from the coastline (5 m) to the same 15 m isobath (Table 1 and Fig. 8). The convergence at 15 m water depth corresponds to a zone with organic matter accumulation. The coastal zone is a shallow water area with high-energy swell and weak tidal currents. In the deeper offshore area, the situation is reversed, with tidal currents is more energetic than the swell. Between these two zones, at 15 m depth, the energy is reduced to a minimum, giving rise to an increase in sediment organic matter content (Fig. 9). The maximum TOC concentration corresponds to the limit between areas with prevailing swell/tide action as defined by Larsonneur (1971) in the bay of Veys (France), which is situated to the west of the Bay of Seine.

On the other hand, a similar pattern can be observed farther south-west, in a smaller area with a less marked TOC gradient. The TOC concentrations are lower than in the NE for the same depth (Fig. 8 and 9), probably in relation with a higher energy hydrodynamic regime. Bottom current velocities in this sector (Fig. 2, location 3) are higher, in contrast to values measured in the NE sector (location 5 and 6).

The TOC gradient in the NE sector shown on Fig. 8 is linked to swell action and tidal processes, in relation to bathymetric control. At the limit between prevailing swell/tide action, the energy is lower and the sediment are richer in TOC (Fig. 8 and 9). The sedimentary state in this area was in dynamic equilibrium (at the time of sampling). It is possible to distinguish another area in dynamic equilibrium located farther to the SW, but it is smaller in size and poorer in organic matter, probably due to higher-energy hydrodynamics.

5.2. Disturbance

Sediment in the harbour basins and the eastern Bay of Seine are the result of mixing between estuarine and marine sources. The common influence of these two sources makes it difficult to discriminate dumped sediment from natural deposits based on classical geochemical markers of the origin of the particulate matter. However, harbour basins are a protected semi-open area, where the sediment are enriched in fine particles associated with intense sulphate-reduction processes. These sediment display high contents in Rb, TOC and S, especially in the deeper samples. They also show higher Pb contents, due to the presence of large quantities of

this element in the Seine estuary (>100 ng l^{-1}) and its capacity to become easily and rapidly fixed to sulphides (Cossa et al., 1993). However, anoxic dumped sediment are quickly re-oxygenated and lose sulphides, lead and part of their fine fraction content. Finally, particles transported around the dumping site remain finer over time and are more organic-rich than the natural sediment that stays in a dynamic equilibrium state. Thus, the structured pattern of TOC gradients allows us to delimit the area disturbed by the dumped dredge spoil. Within this disturbed area, TOC gradients converge towards the dumping site (Fig. 8).

Thus, it is possible to monitor the spatial distribution of dumped sediment and delimit areas under anthropogenic influence by using a dynamic tracer such as TOC.

5.3. Synthesis

Fig. 10 summarizes the three main areas with their specific characteristics.

In the NE, sediment are in dynamic equilibrium and display two gradients related to the bathymetry which converge towards 15 m depth. Tidal currrents prevail offshore, while swell is dominant in the coastal zone. In these two domains, sediment are mainly organic-poor sands in accordance with the strong hydrodynamics. The maximum TOC concentration at 15 m depth picks out the limit between the prevailing action of swell or tide that corresponds to the minimum energy.

Another area farther SW is not impacted by dumping, but the dynamic equilibrium state is different from the NE sector despite the same water depth. The sandy composition of sediment prevents the use of TOC as a dynamic tracer.

Finally, the central area corresponds to a zone disturbed by the dumping site. The dumping causes morphological changes such as the formation of a dome (-5m CMH) SE of the dumping site. This dome, which is close to the coast, impacts the trajectory and intensity of tidal currents, leading to the accumulation of organic-poor sands. The dumping of sediment also contributes to the injection of particulate matter derived from the harbour. According to our results, the particles deposited at the dumping site are dispersed by currents which follow three directions. A first component is driven to the NE, without significantly impacting the area showing TOC gradients. A second component is evacuated offshore to the north without permanent accumulation. The third component appears to be dispersed southwards. However, it is difficult to determine the origin of these materials, which could be derived from the Seine estuary, or could represent resuspended particles from the navigation channel or from other anthropogenic sources.

Thus, this innovative approach uses concentration gradients of geochemical tracers to study the dynamic equilibrium of sedimentation and allows us to identify a disturbed area and the main pathways for the dispersal of dumped sediment in the eastern part of the Bay of Seine. This anthropogenic area modifies the natural dynamic equilibrium. It will be interesting to apply this new method to other dumping sites in coastal areas, within the Bay of Seine or elsewhere, which show similar physical and sedimentological characteristics.

Acknowledgments

The results in this study come from the PhD thesis of N. Baux. The authors are grateful to the Grand Port Maritime du Havre for financing the CIFRE thesis, as well as data sharing and the provision of a research vessel. We wish to thank the crews of “Le Marais” and “Le Côtes de la Manche”, as well as the Flavie Druine, for their help during sampling. We wish to thank the staff of the M2C Laboratory (particularly M. Legrain, C. Thouroude and C. Brunaud) and the staff of CNAM-Intechmer laboratory, for assistance in technical operations. We would like to express our gratitude to M. Carpenter for post-editing the English style and grammar. Finally, we also thank both reviewers for their useful comments on the first version of this paper.

References

Auffret, J. and d'Ozouville, L. (1985a). Apports de l'imagerie fournie par le sonar à balayage latéral à la connaissance de la dynamique sédimentaire en Baie de Seine. Actes de colloque IFREMER, 4:201-210.

Auffret, J. and d'Ozouville, L. (1985b). Cartographie du prisme sédimentaire holocène en baie de Seine orientale, par sismique réflexion à haute définition. Actes de colloque IFREMER, 4:109-116.

Avoine, J., Allen, G. P., Nichols, M., Salomon, J. C., and Larsonneur, C. (1981). Suspended-sediment transport in the Seine estuary, France: effect of man-made modifications on estuary-shelf sedimentology. Marine Geology, 40(1-2):119-137.

Avoine, J. and Larsonneur, C. (1987). Dynamics and behaviour of suspended sediment in macrotidal estuaries along the south coast of the English Channel. *Continental Shelf Research*, 7(11-12):1301-1305.

Banerjee, S., Bansal, U., and Vilas Thorat, A. (2016). A review on palaeogeo-graphic implications and temporal variation in glaucony composition. Journal of Palaeogeography, 5(1):43-71.

Barringer, J. L., Mumford, A., Young, L. Y., Reilly, P. A., Bonin, J. L., and Rosman, R. (2010). Pathways for arsenic from sediments to groundwater to streams: Biogeochemical processes in the Inner Coastal Plain, New Jersey, USA. Water Research, 44(19):5532-5544.

Barringer, J. L., Szabo, Z., Barringer, T. H., and Holmes, C. W. (2001). Mobility of arsenic in agricultural and wetlands soils and sediments, Northern Coastal Plain of New Jersey. US Geological Survey Report. Retrieved March , 7:12013.

Bo Barker, J. (1977). The sulfur cycle of a coastal marine sediment (Limfjorden, Denmark). Limnology and Oceanography , 22:814-832.

Boutin, R. (2000). Amélioration des connaissances sur les rejets par clapage de type vase. VI^{èmes} Journées Nationales Génie Civil - Génie Côtier, Caen, France (17-19 Mai 2000). 623-633.

Bracken, L. J. and Wainwright, J. (2006). Geomorphological equilibrium: myth and metaphor? Transactions of the Institute of British Geographers, 31(2):167-178.

Brasselet, S. (2014). Dragages d'entretien du Grand Port Maritime du Havre. Arrêté inter préfectoral du 26/10/2009 : Renouvellement de l'autorisation de dragage et de l'immersion des produits de dragages d'entretien du GPMH. Demande de renouvellement. Rapport interne. Grand Port Maritime du Havre (GPMH) - Service Accès et Environnement Maritime, (2014-080-A). 1-233.

Brylinski, J.-M., Lagadeuc, Y., Gentilhomme, V., Dupont, J. P., Lafite, R., Dupeuble, P.-A., Huault, M.-F., Auger, Y., Puskaric, E., Wartel, M., and Cabioch, L. (1991). Le "fleuve côtier" : un phénomène hydrologique important en Manche orientale : Exemple du Pas-de-Calais. Oceanologica Acta, SP(11):197-203.

Chauvin, P., Freger, G., and Guyader, J. (1986). Synthèse des connaissances sur les effets du dépôt de dragage d'Octeville. Acte de colloque IFREMER, 4:465-470.

Christie, M. C., Dyer, K. R., and Turner, P. (1999). Sediment flux and bed level measurements from a macrotidal mudflat. Estuarine, Coastal and Shelf Science, 49(5):667-688.

Cossa, D., Elbaz-Poulichet, F., Gnassia-Barelli, M., and Romeo, M. (1993). Le plomb en milieu marin. Biogeochimie et écotoxicologie. Repères Océan, 3:1-377.

Crevel, L. (1985). La dynamique sédimentaire en Baie de Seine nord-orientale, fluctuations et évolution de la couverture meuble. Actes de colloque IFRE-MER, 4:193-200.

Dubrulle, C., Lesueur, P., Boust, D., Dugué, O., Poupinet, N., and Lafite, R. (2007). Source discrimination of fine-grained deposits occurring on marine beaches: The Calvados beaches (eastern Bay of the Seine, France). Estuarine, Coastal and Shelf Science, 72(1):138-154.

Dubrulle-Brunaud, C. (2007). Les sédiments fins dans un système macrotidal actuel (continuum Seine-Baie de Seine) : caractérisation géochimiques et minéralogiques, identification des sources. Thèse de doctorat. Université de Rouen.1-1341.

Dupont, J. P., Lafite, R., Huault, M. F., Hommeril, P., and Meyer, R. (1994). Continental/marine ratio changes in suspended and settled matter across a macrotidal estuary (the Seine estuary, northwestern France). Marine Geology, 120(1):27-40.

Dyer, K. R., Christie, M. C., and Wright, E. W. (2000). The classification of intertidal mudflats. Continental Shelf Research, 20(10):1039-1060.

Elineau, S. (2013). Le risque naturel côtier sur la communauté d'agglomération du Havre (Haute-Normandie) : Une évaluation des aléas. Thèse de doctorat. Le Havre Université. 1-1297.

Garrels, R. M. and Christ, C. L. (1965). Solutions, minerals, and equilibria. Harper & Row. New York.

Gilbert, G. (1877). Report on the geology of the Henry Mountains. United States Geographical and Geological Survey of the Rocky Mountains Region. Washington, DC.

Goldberg, E. D., Grin, J. J., Hodge, V., Koide, M., and Windom, H. (1979). Pollution history of the Savannah River estuary. Environmental Science & Technology, 13(5):588-594.

Hotelling, H. (1933). Analysis of a complex of statistical variables into principal components. Journal of Educational Psychology, 24:417-520.

Jørgensen, B. B. (1977). The sulfur cycle of a coastal marine sediment (Limfjorden, Denmark). Limnology and Oceanography, 22(5):814-832.

Kasten, S. and Jørgensen, B. B. (2000). Sulfate Reduction in Marine Sediments.
Marine Geochemistry, eBook: 263-281.

Larsonneur, C. (1971). Manche centrale et baie de Seine : géologie du substratum et des dépôts meubles. Thèse d'Etat, Université de Caen. 1-1394.

Larsonneur, C., Auffret, J., and Avoine, J. (1985). Etudes hydrosédimentaires en Baie de Seine. Rapport final, 83/7163:1-80.

Larsonneur, C., Horn, R., Auffret, J. P., Hommeril, P., Moal, A., and (1975). Géologie de la partie méridionale de la Manche centrale. Phil. Trans. R. Soc. Lond. A, 279(1288):145-153.

Le Hir, P., Ficht, A., Jacinto, R. S., Lesueur, P., Dupont, J.-P., Lafite, R., Brenon, I., Thouvenin, B., and Cugier, P. (2001a). Fine sediment transport and accumulations at the mouth of the Seine estuary (France). Estuaries, 24(6):950-963.

Le Hir, P., Lesueur, P., Alart, D., and Abarnou, A. (2001b). Contextes climatique, morphologique et hydro-sédimentaire : dynamique des matériaux fins dans l'estuaire de la seine. Rapport d'étude. Gip Seine-Aval. 1-6.

Lee, S. V. and Cundy, A. B. (2001). Heavy metal contamination and mixing processes in sediments from the Humber Estuary, Eastern England. Estuarine, Coastal and Shelf Science, 53(5):619-636.

Leri, A. C., Hakala, J. A., Marcus, M. A., Lanzirotti, A., Reddy, C. M., and Myneni, S. C. B. (2010). Natural organobromine in marine sediments: New evidence of biogeochemical Br cycling. Global Biogeochemical Cycles, 24(4): 40-17.

Leri, A. C., Mayer, L. M., Thornton, K. R., and Ravel, B. (2014). Bromination of marine particulate organic matter through oxidative mechanisms. Geochimica et Cosmochimica Acta, 142:53-63.

Lesourd, S. (2000). Processus d'envasement d'un estuaire macrotidal : zoom temporel du siècle à l'heure ; application à l'estuaire de la seine. Thèse de doctorat. Université de Caen Basse-Normandie. 1-1303.

Lesourd, S., Lesueur, P., Brun-Cottan, J. C., Garnaud, S., and Poupinet, N. (2003). Seasonal variations in the characteristics of superficial sediments in a macrotidal estuary (the Seine inlet, France). Estuarine, Coastal and Shelf Science, 58(1):3-16.

Lesourd, S., Lesueur, P., Fisson, C., and Dauvin, J. C. (2016). Sediment evolution in the mouth of the Seine estuary (France): A long-term monitoring during the last 150 years. Comptes Rendus Geoscience, 348(6):442-450.

Lewis, P. D. and Menzies, G. E. (2015). Vibrational spectra, principal components analysis and the horseshoe effect. Vibrational Spectroscopy, 81:62-67.

Macdonald, R. W., Macdonald, D. M., O'Brien, M. C., and Gobeil, C. (1991). Accumulation of heavy metals (Pb, Zn, Cu, Cd), carbon and nitrogen in sediments from Strait of Georgia, B.C., Canada. Marine Chemistry, 34(1):109-135.

Mahjoor, A., Karimi, M., and Rastegarlari, A. (2009). Mineralogical and geochemical characteristics of clay deposits from South Abarkouh district of clay deposit (Central Iran) and their applications. Journal of Applied Sciences, 9(4):601-614.

Méar, Y., Poizot, E., Murat, A., Beryouni, K., Baux, N., and Dauvin, J.-C. (2018). Improving the monitoring of a dumping site in a dynamic environment. Example of the Octeville site (Bay of Seine, English Channel). Marine Pollution Bulletin, 129(2):425-437.

Méar, Y., Poizot, E., Murat, A., Lesueur, P., and Thomas, M. (2006). Fine-grained sediment spatial distribution on the basis of a geostatistical analysis: Example of the eastern Bay of the Seine (France). Continental Shelf Research, 26(19):2335-2351.

Marmin, S., Dauvin, J., and Lesueur, P. (2014). Collaborative approach for the management of harbour-dredged sediment in the Bay of Seine (France). Ocean and Coastal Management, 102:328-339.

Marmin, S., Lesueur, P., Dauvin, J. C., Samson, S., Tournier, P., Gallicher La-vanne, A., Dubrulle-Brunaud, C., and Thouroude, C. (2016). An experimental study on dredge spoil of estuarine sediments in the bay of seine (France): A morphosedimentary assessment. Continental Shelf Research, 116:89-102.

Mayer, L. M., Macko, S. A., Mook, W. H., and Murray, S. (1981). The distribution of bromine in coastal sediments and its use as a source indicator for organic matter. Organic Geochemistry, 3(1):37-42.

Mayer, L. M., Schick, L. L., Allison, M. A., Ruttenberg, K. C., and Bentley, S. J. (2007). Marine vs. terrigenous organic matter in Louisiana coastal sediments: The uses of bromine:organic carbon ratios. Marine Chemistry, 107(2):244-254.

McRae, S. G. (1972). Glauconite. Earth-Science Reviews, 8(4):397-440.

Mumford, A. C., Barringer, J. L., Benzel, W. M., Reilly, P. A., and Young, L. Y. (2012). Microbial transformations of arsenic: Mobilization from glauconitic sediments to water. Water Research, 46(9):2859-2868.

Murat, A., Méar, Y., Poizot, E., Dauvin, J., and Beryouni, K. (2016). Silting up and development of anoxic conditions enhanced by high abundance of the geo-engineer species Ophiothrix fragilis. Continental Shelf Research, 118:11-22.

Oliveira, A., Rocha, F., Rodrigues, A., Jouanneau, J., Dias, A., Weber, O., and Gomes, C. (2002). Clay minerals from the sedimentary cover from the Northwest Iberian shelf. Progress in Oceanography, 52(2):233-247.

Pearson, K. (1901). On lines and planes of closest fit to systems of points in space. The London, Edinburgh, and Dublin Philosophical Magazine and Journal of Science, 2(11):559-572.

Perillo, G. M. E. (1995). Chapter 1 Geomorphology and sedimentology of estuaries: An Introduction. Developments in Sedimentology. Elsevier, 53:1-16.

Price, N. B. and Calvert, S. E. (1977). The contrasting geochemical behaviours of iodine and bromine in recent sediments from the Namibian shelf. Geochimica et Cosmochimica Acta, 41(12):1769-1775.

Reynolds, R. C. (1963). Potassium-rubidium ratios and polymorphism in illites and microclines from the clay size fractions of proterozoic carbonate rocks. Geochimica et Cosmochimica Acta, 27(11):1097-1112.

Santschi, P. H., Guo, L., Asbill, S., Allison, M., Britt Kepple, A., and Wen, L.-S. (2001). Accumulation rates and sources of sediments and organic carbon on the Palos Verdes shelf based on radio-isotopic tracers (137cs, 239,240pu, 210pb, 234th, 238u and 14c). Marine Chemistry, 73(2):125-152.

Shaw, T. J., Gieskes, J. M., and Jahnke, R. A. (1990). Early diagenesis in differing depositional environments: the response of transition metals in pore water. Geochimica et Cosmochimica Acta, 54(5):1233-1246.

Smith, S. D. A. and Rule, M. J. (2001). The effects of dredge spoil dumping on a shallow water soft-sediment community in the Solitary Islands Marine Park, NSW, Australia. Marine Pollution Bulletin, 42(11):1040-1048.

Spencer, K. L., Cundy, A. B., and Croudace, I. W. (2003). Heavy metal distribution and early-diagenesis in salt marsh sediments from the Medway Estuary, Kent, UK. Estuarine, Coastal and Shelf Science, 57(1-2):43-54.

Syms, C. (2008). Principal Components Analysis. Encyclopedia of Ecology. Jørgensen, Sven Erik and Fath, Brian D. 2940-2949.

Ubertini, M., Lefebvre, S., Gangnery, A., Grangeré, K., Le Gendre, R., and Orvain, F. (2012). Spatial Variability of Benthic-Pelagic Coupling in an Estuary Ecosystem: Consequences for Microphytobenthos Resuspension Phenomenon. Plos One, 7(8):1-17.

Vrel, A. (2012). Reconstitution de l'historique des apports en radionucléides et contaminants métalliques à l'estuaire fluvial de la seine par l'analyse de leur enregistrement sédimentaire. Thèse de doctorat. Université de Caen Basse-Normandie.1-344.

Figures

Figure 1: Study area with inset showing Le Havre harbour and current measurement sites. Bathymetry data from SHOM (1996) and Le Havre harbour (2016).

Figure 2: Multi-scale study areas with overall view and insets showing two zones. Zoom 1: samples from Seine estuary; Zoom 2: samples from harbour basins. Triangles: samples from strongly dredged basins; Stars: samples from slightly basins; Squares: grab samples of dredged sediment; Underlined text: samples from Port 2000.

Figure 3: Results of final PCA with interpretations. A: representation of variables; B: representation of samples.

Figure 4: Correlation matrix, with values of coefficient for pairs of elements. * p-value 0.1 %, ** p-value 0.05 and ***: p-value 0.01%

Figure 5: A: Relation between Rb (ppm) and mean particle size (µm) for the three groups identified in figure 3; B: Relation between Rb (ppm) and TOC (%) for the three groups identified in figure 3.

Figure 6: Results of PCA applied to samples of Blue group.

Figure 7: Cartographic representation of geochemical results. Colour coding according to groups and sub-groups defined in figure 3B.

Figure 8: Map showing TOC concentrations and gradients with delimitation of areas with sedimentary state in dynamic equilibrium.

Figure 9: Depth (m) versus TOC (%), with interpretations, for samples located in an area with a TOC gradient (NE sector of study area; figure 8).

Figure 10: Summary map and interpretations with delimitation of areas in dynamic equilibrium and disturbed areas.

Tables

Table 1: Mean contents of the geochemical parameters (in ppm for As, Rb, BrOrg, Sulphide and Pb; in % for Si and TOC), for each group and sub-group identified from PCA results. In addition, mean particle size (<2000 µm) measured with laser diffraction analyzer (data in µm) and number of samples contained in groups and sub-groups. In bold, mean for each group. bdl: below detection limits.

Table 2: Mean bottom current velocities (m s^{-1}) and associated bathymetric data (with respect to CMH datum) from Le Havre harbour study (Brasselet, 2014), during spring and neap tides. Measuring points located on figure 1.

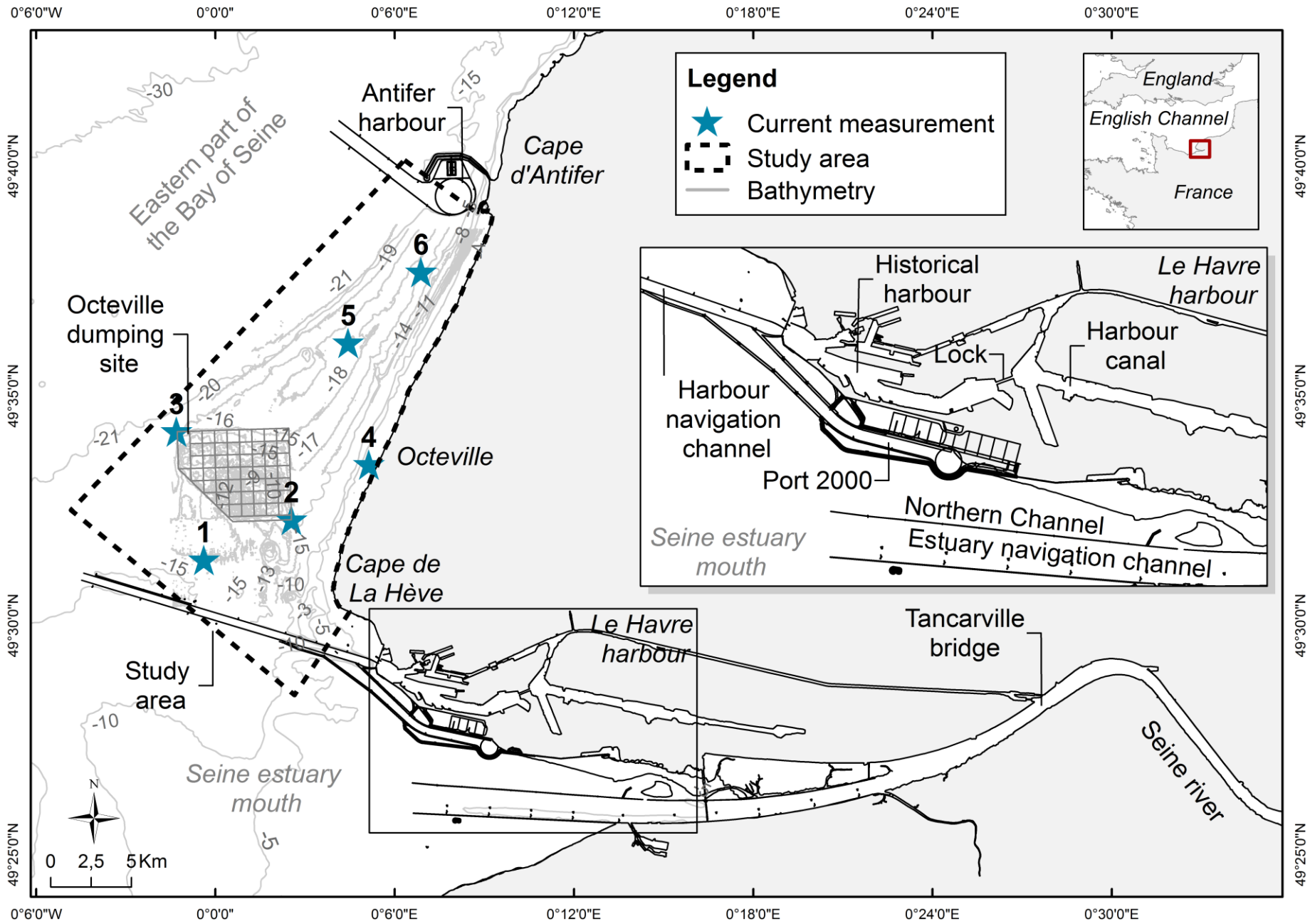

Fig. 1: Study area with inset showing Le Havre harbour and current measurement sites. Bathymetry data from SHOM (1996) and Le Havre harbour (2016).

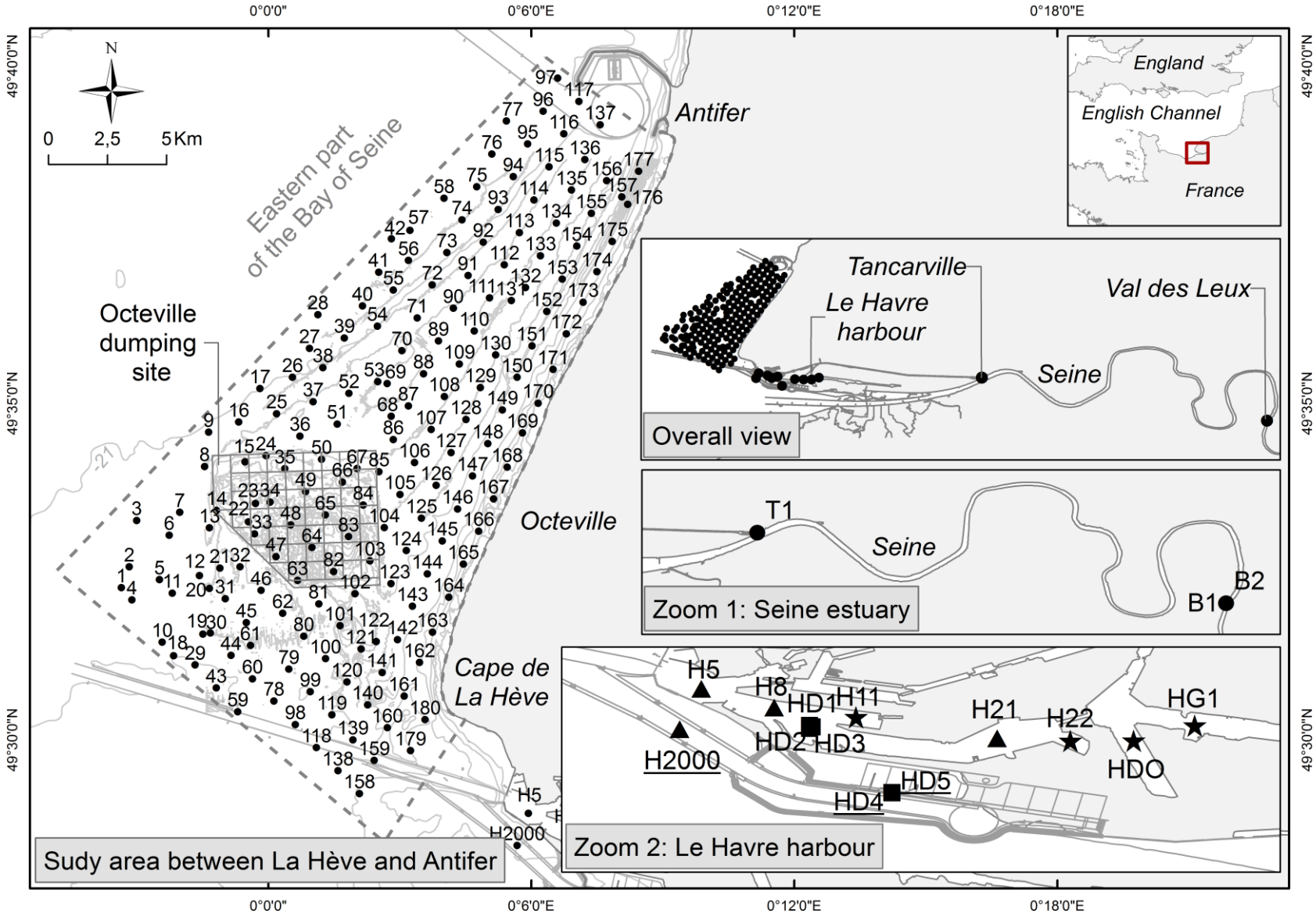

Fig. 2: Multi-scale study areas with overall view and insets showing two zones. Zoom 1: samples from Seine estuary; Zoom 2: samples from harbour basins. Triangles: samples from strongly dredged basins; Stars: samples from slightly basins; Squares: grab samples of dredged sediment; Underlined text: samples from Port 2000.

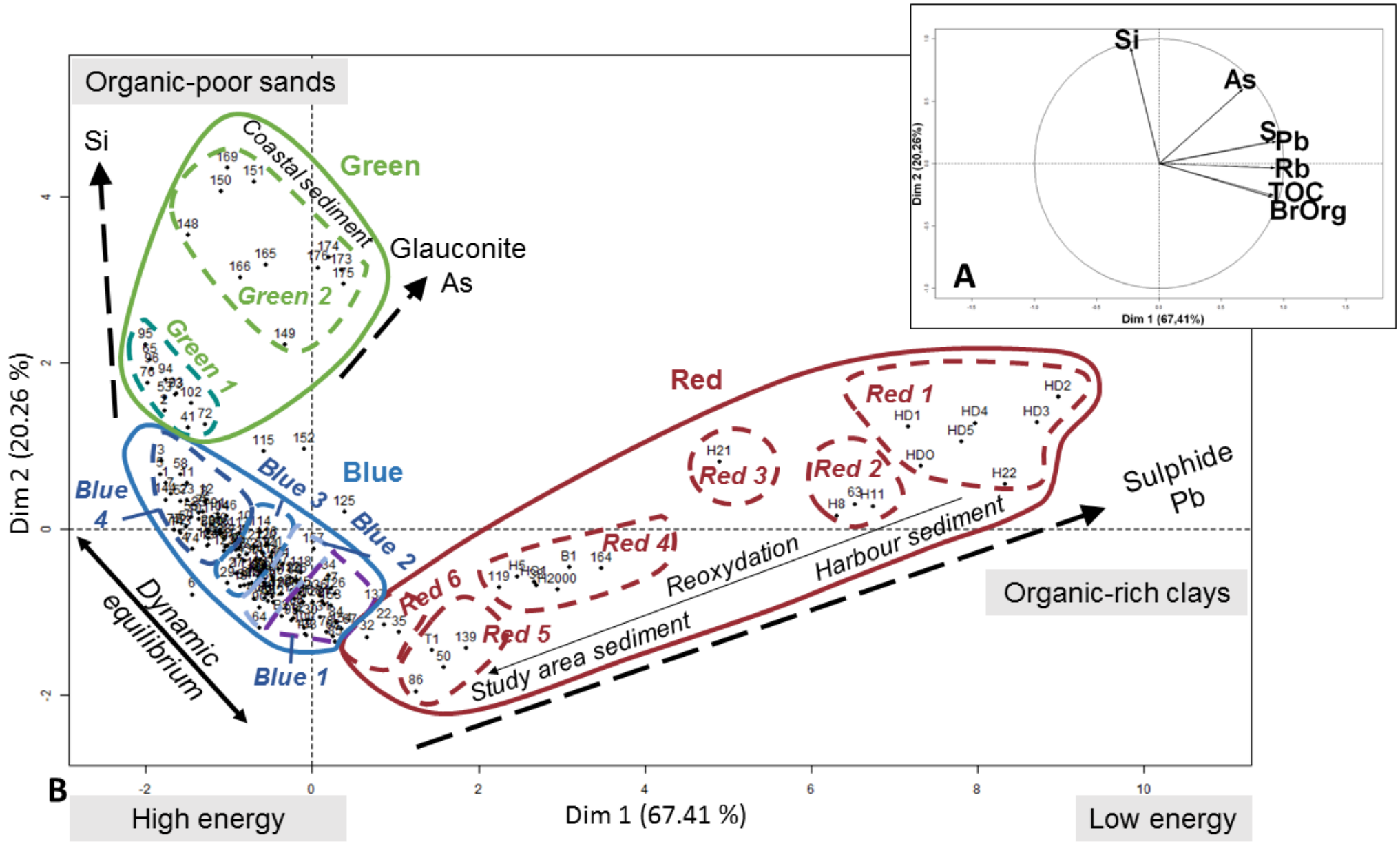

Fig. 3: Results of final PCA with interpretations. A: representation of variables; B: representation of samples.

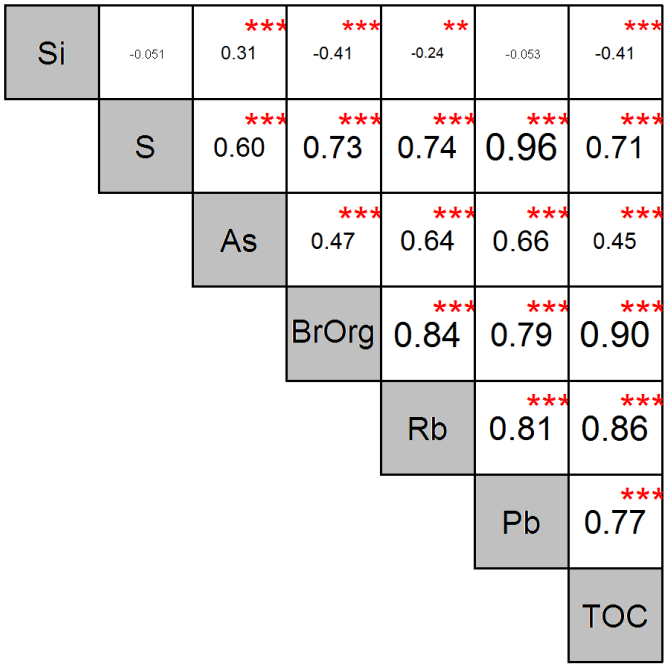

Fig. 4: Correlation matrix, with values of coefficient for pairs of elements. * p-value 0.1 %, ** p-value 0.05 and ***: p-value 0.01%

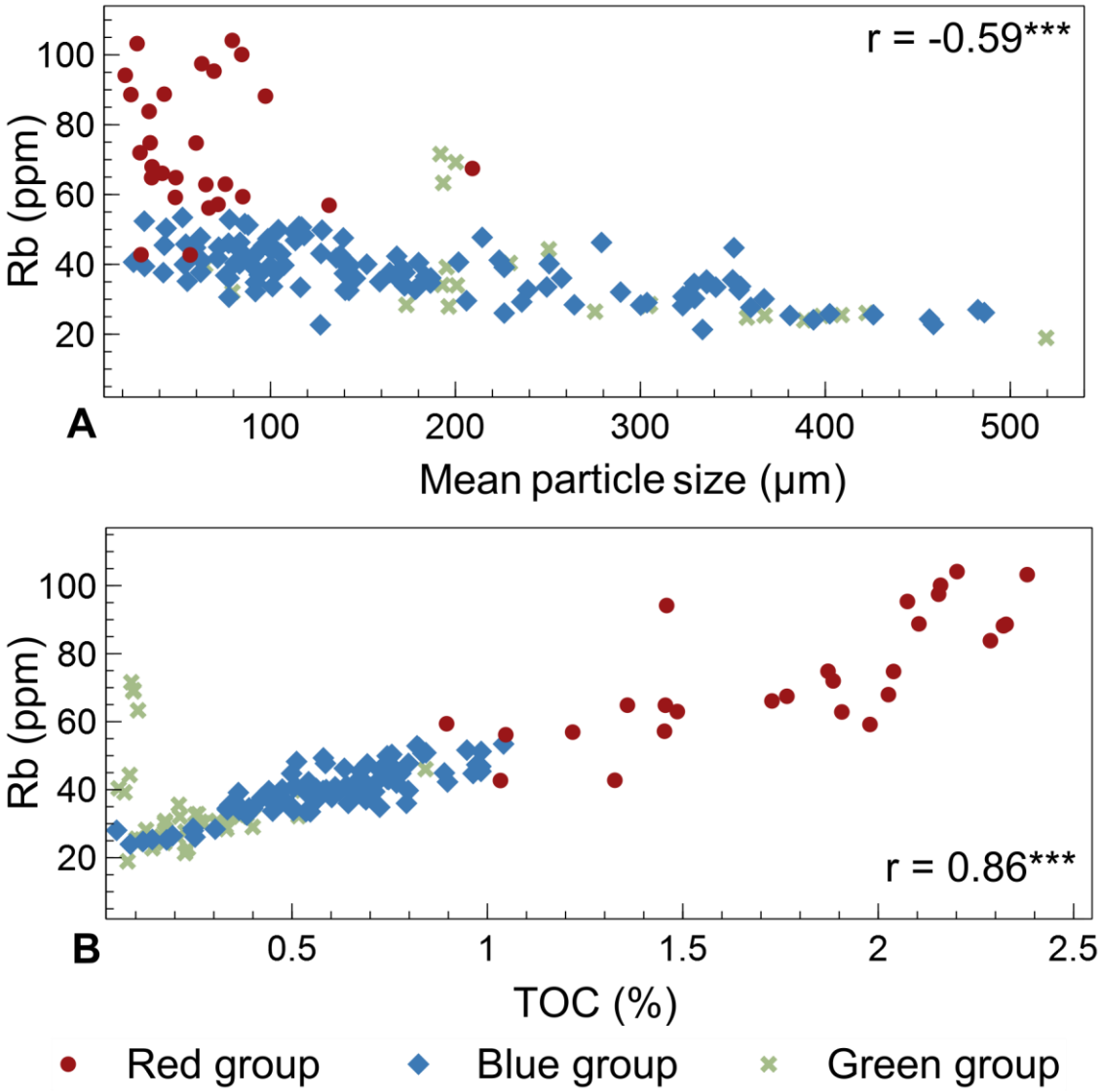

Fig. 5: A: Relation between Rb (ppm) and mean particle size (µm) for the three groups identified in figure 3; B: Relation between Rb (ppm) and TOC (%) for the three groups identified in figure 3.

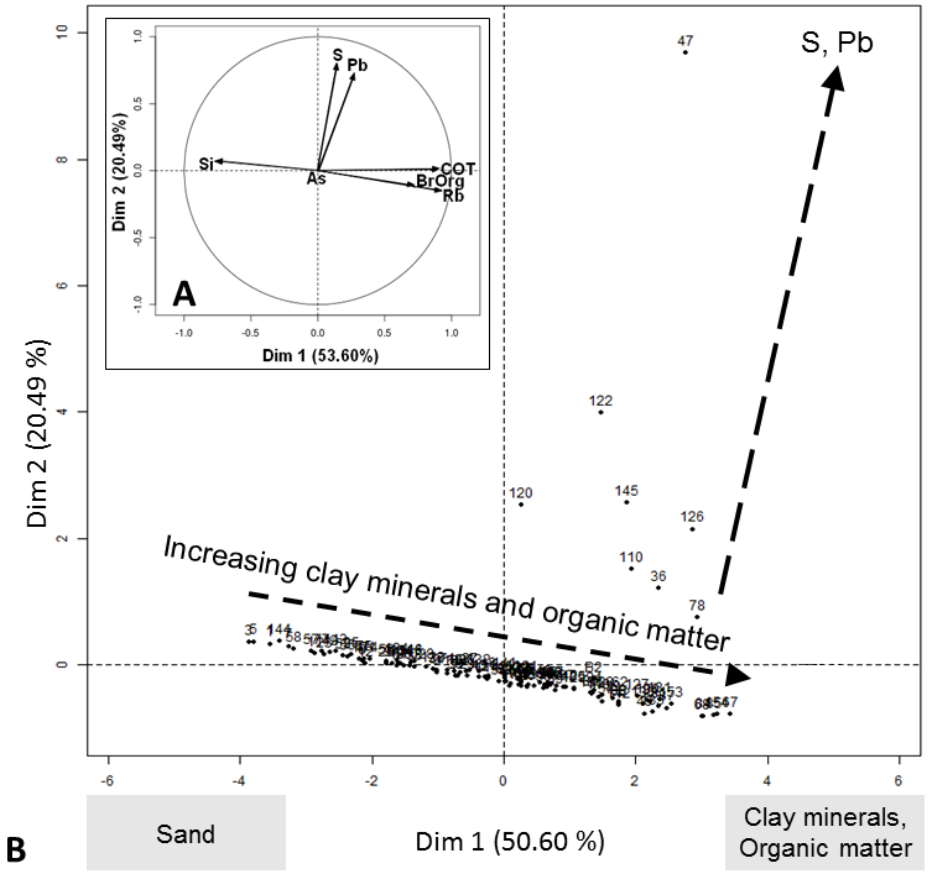

Fig. 6: Results of PCA applied to samples of Blue group.

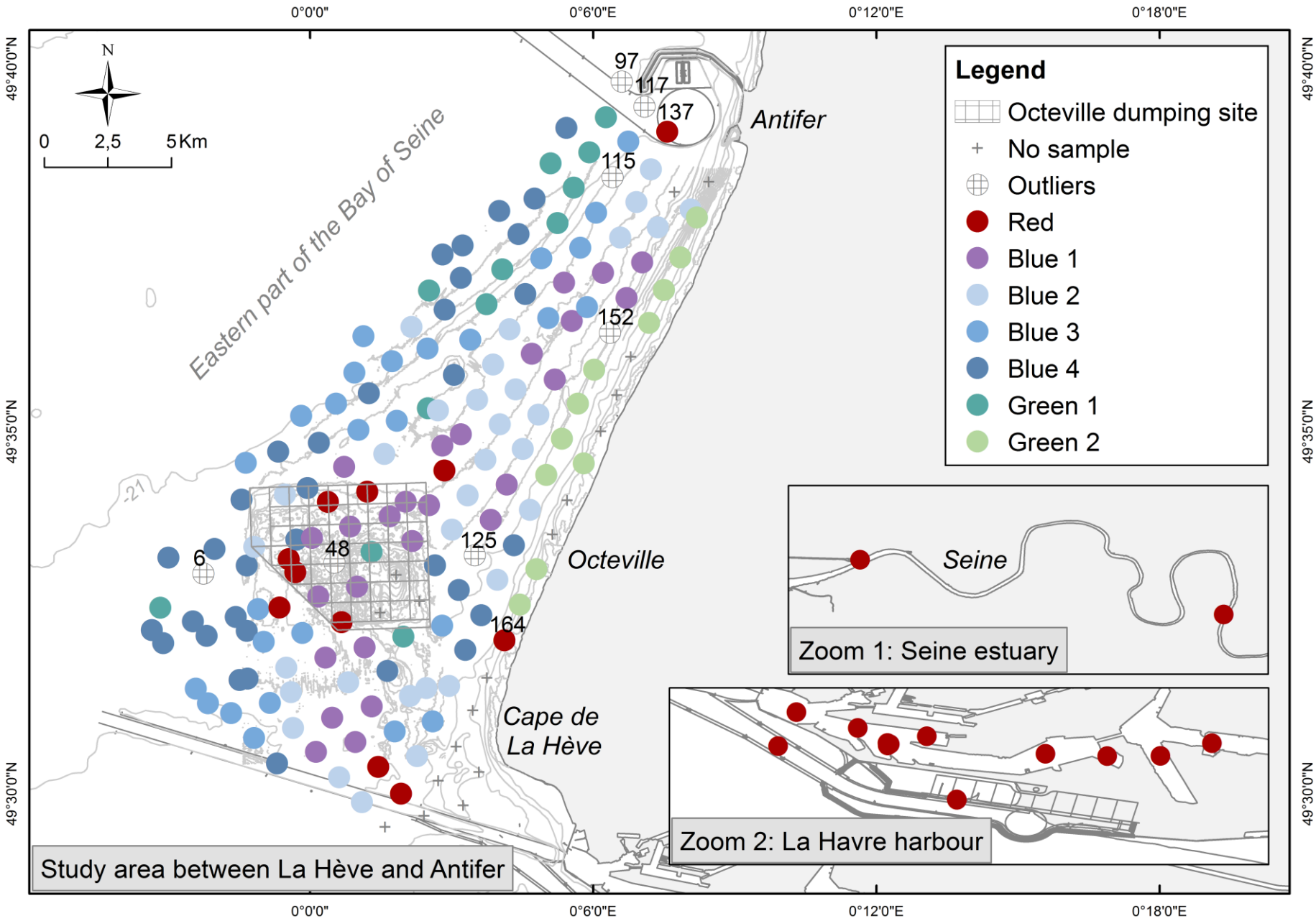

Fig. 7: Cartographic representation of geochemical results. Colour coding according to groups and sub-groups defined in figure 3B.

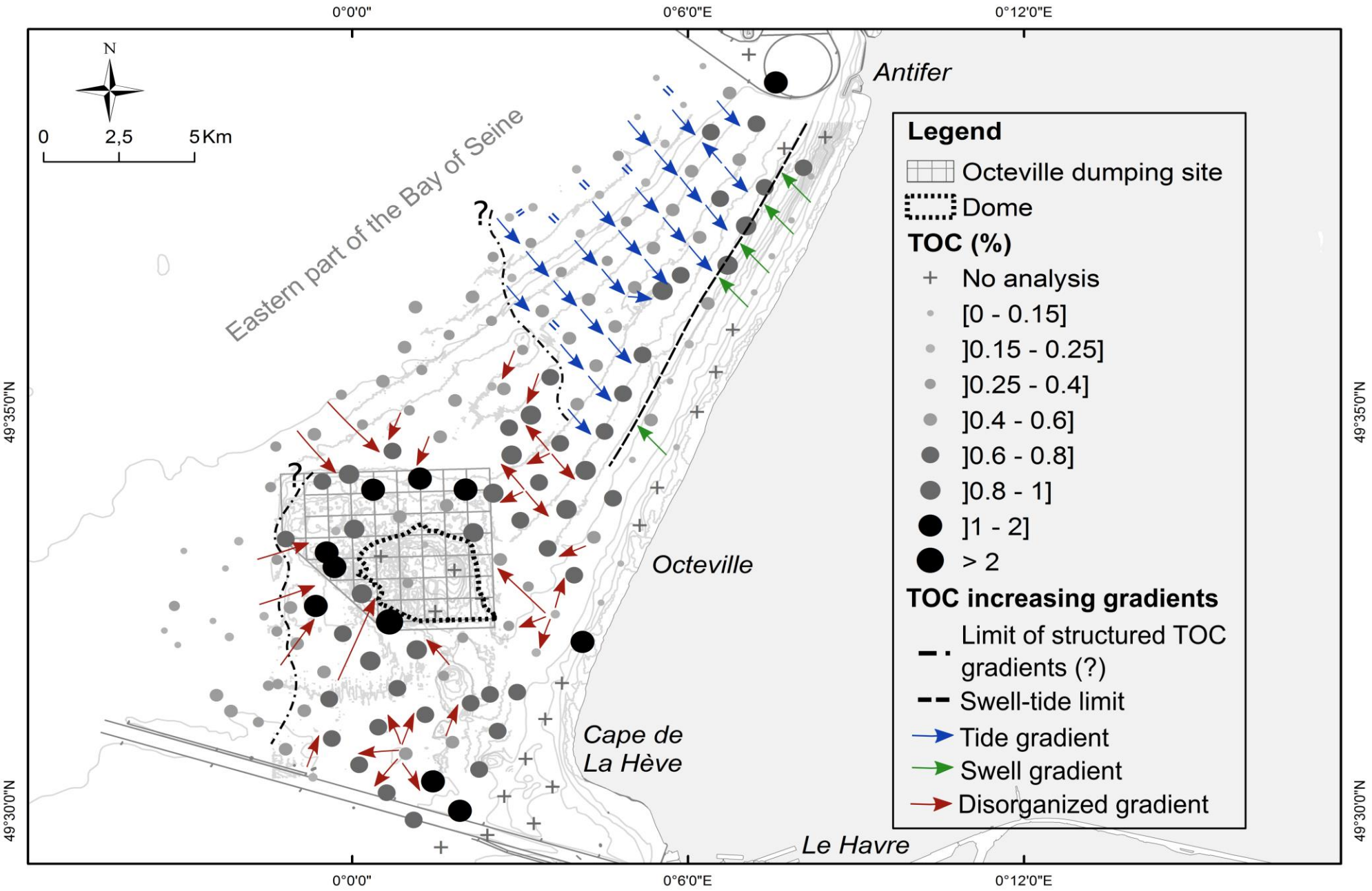

Fig. 8: Map showing TOC concentrations and gradients with delimitation of areas with sedimentary state in dynamic equilibrium.

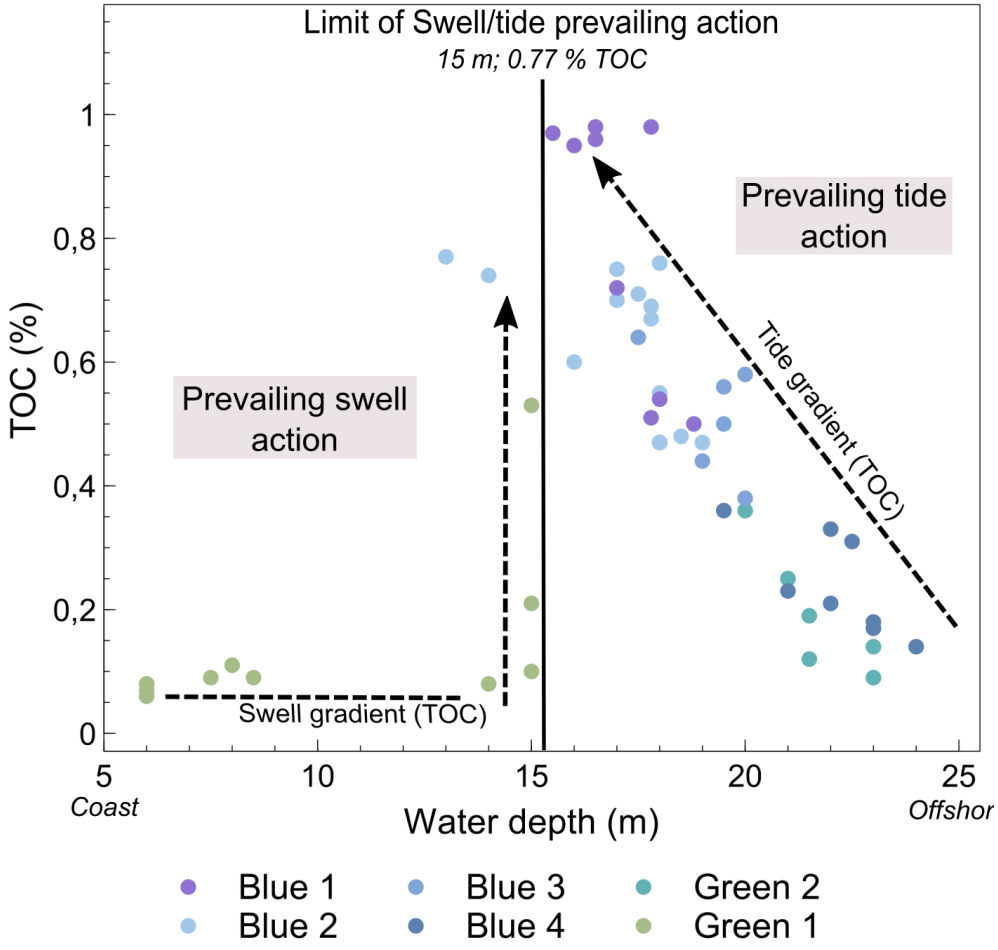

Fig. 9: Depth (m) versus TOC (%), with interpretations, for samples located in an area with a TOC gradient (NE sector of study area; Fig. 8)

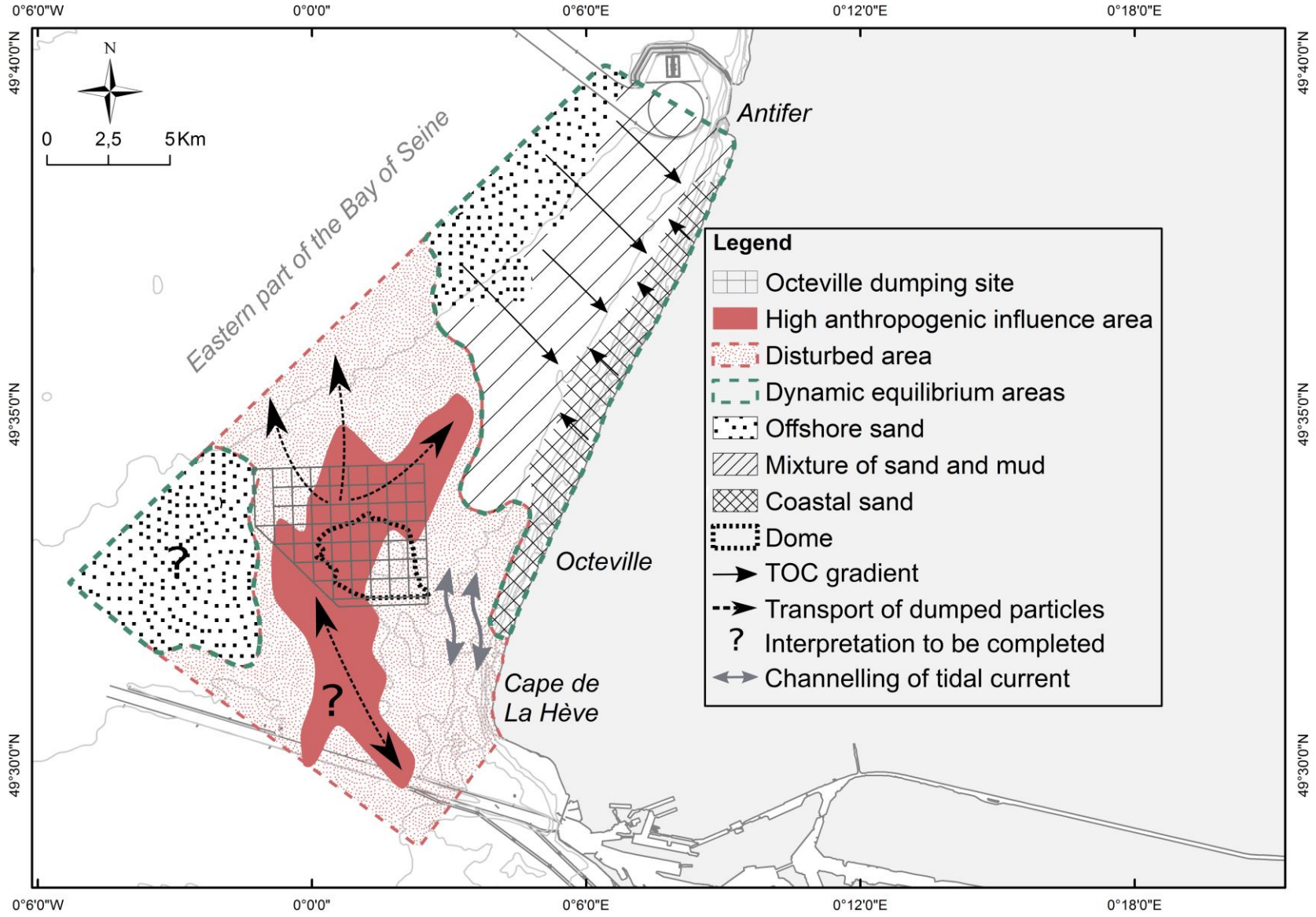

Figure 10: Summary map and interpretations with delimitation of areas in dynamic equilibrium and disturbed areas.

Table 1: Mean contents of the geochemical parameters (in ppm for As, Rb, BrOrg, Sulphide and Pb; in % for Si and TOC), for each group and sub-group identified from PCA results. In addition, mean particle size (<2000 µm) measured with laser diffraction analyzer (data in µm) and number of samples contained in groups and sub-groups. In bold, mean for each group. Bdl: below detection limits.

	Number	**Si**	**As**	**Rb**	**BrOrg**	**TOC**	**S**	**Pb**	**Particle size**
Red1	7	25.29	11	95	141	2.19	6243	93	69
Red2	3	23.93	8	87	126	2.24	4266	73	34
Red3	1	23.47	10	68	58	2.03	4084	63	36
Red4	7	21.92	6	**71**	77	1.67	582	21	40
Red5	4	21.14	Bdl	62	71	1.53	Bdl	12	105
Red6	4	22.65	Bdl	53	57	1.26	248	6	75
Red	**26**	**23.11**	**6**	**75**	**95**	**1.80**	**2525**	**44**	**62**
Blue1	27	22.03	Bdl	47	45	0.77	99	1	100
Blue2	32	23.48	Bdl	**41**	31	0.65	Bdl	1	121
Blue3	27	24.49	Bdl	36	24	0.49	Bdl	Bdl	180
Blue4	34	25.96	Bdl	29	11	0.28	Bdl	bdl	287
Blue	**120**	**24.08**	**Bdl**	**38**	**27**	**0.54**	**22**	**1**	**177**
Green1	12	33.93	Bdl	28	6	0.21	Bdl	Bdl	299
Green2	11	35.53	10	47	2	0.14	Bdl	5	212
Green	**23**	**34.69**	**5**	**37**	**4**	**0.18**	**Bdl**	**2**	**257**

Table 2: Mean bottom current velocities (m s^{-1}) and associated bathymetric data (with respect to CMH datum) from Le Havre harbour study (Brasselet, 2014), during spring and neap tides. Measuring points located on figure 1.

Measurement points	State of tide	Bathymetry	Mean speeds	Max speeds
1	Sping tide	-14	0.35	0.56
	Neap tide	-14	0.15	0.24
2	Sping tide	-13	0.37	0.66
	Neap tide	-13	0.15	0.27
3	Sping tide	-17	0.40	0.62
	Neap tide	-17	0.22	0.29
4	Sping tide	-1	0.25	0.47
	Neap tide	-	-	-
5	Sping tide	-16	0.36	0.58
	Neap tide	-16	0.20	0.31
6	Sping tide	-15	0.27	0.50
	Neap tide	-15	0.15	0.26